

# Intuitive physics leads to epidemic models: Focus on smallpox

DRAFT 01 June 2004

R. Crandall\*, G. Oxman\*\*, M. Helman\*\*, and A. Sullivan\*\*

**Abstract.** We provide pedagogical avenues for the transition from stochastic-physics models, for example intuitive models of conflagration (e.g. forest fires), to sophisticated epidemic models. We focus on the case of smallpox, indicating both discrete and continuum approaches. We pay attention to fundamental differences between such approaches, in regard to survivor sets and spatial conflagration (infection) boundaries. In particular, we observe that continuum (differential) models convey useful and time-honored results, yet detailed questions as pertain to vaccination strategies and classification of epidemics should rely on the discrete pictures which, indeed, can yield surprising results such as evident fractal structure of both survivor sets and ongoing epizootic wavefronts.

\* Center for Advanced Computation, Reed College

\*\* Multnomah County (Oregon) Health Department

## 1. Introduction

In recent times especially, smallpox-outbreak and other epidemic models abound [1]. For the purpose of the present treatment, we group such models into two basic varieties: Discrete and continuum—although as we shall see, discrete models can be further divided into basic classes. Later we shall specify precise discretizations of time and/or space coordinates, and note that we also put within the "discrete" rubric those models for which incremental probabilities replace diffusive flow. It is perhaps easiest just to imagine the continuum picture as being analytical, i.e. involving differential equations—no matter how intricate or nonlinear—and think of any other picture as discrete.

Continuum models go back at least as far as [Kermack and McKendrick 1927] where the fundamental *SIR* differential system we shall presently derive was formulated, and applied with considerable success to actual disease-outbreak data. Some notable recent works are, let us say first of the discrete variety: [Halloran et al. 2002], [Epstein et al. 2002], [Bozette et al. 2003]; and second, of the continuum variety: [Kaplan et al. 2002]. It should be noted that Bozette et al. work, and others like it, involve phenomenological inferences of a hybrid nature—i.e., with both discrete and continuum elements, such as, say, discrete probabilities but global averages over dense populations and so on.

[ADD: more scholarship on the history and development of smallpox models in particular.]

One cannot possibly cover, without creating a massive review work, the now vast universe of epidemiological models. What we do in this treatment is to provide a pedagogical tour of various carefully chosen models, at every juncture emphasizing methods of theoretical physics, and the intuition usually ascribed to physics thinking. In this way we are presenting an interdisciplinary approach to model development. <sup>1</sup> Nonlinear coupling constants become infection contact rates, microscopic statistical rules lead to specific iterations and classical differential equations, and so on. We touch upon nonlinear phenomena, such as fractal sets and boundaries, and so on.

## 2. Conflagration in the temporal continuum

Perhaps the simplest conflagration model that leads in pedagogical fashion to a practical epidemic model is that of a forest fire, for which we imagine a large, planar areas on which trees live, and denote:

---

<sup>1</sup>In fact, the present research program began when a research group at Reed College joined forces with the Oregon Bioterror Taskforce, in order to understand in an interdisciplinary fashion such as CDC policy and the most recent literature forays into smallpox strategies.

$F(t)$  = number of trees on fire at time  $t$ ,

$G(t)$  = number of green (i.e. not on fire) trees,

$B(t)$  = number of black (i.e. burnt) trees.

Note that, though we may envision a 2-dimensional forest with red, green, and black trees, we are *not* yet invoking spatial dependence; i. e. ,  $F, G, B$  are simply total counts of respective tree states across, say, very large finite region. In an obvious sense we are *integrating* any spatial dependence out of the analysis. If we further envision that the burning trees throw up a “cinder storm”—so that any burning tree threatens every green tree in a uniform (spatially-independent) sense—then the rate of ignition of green  $\rightarrow$  red is reasonably assumed to be proportional to the product  $FG$ . Furthermore we assume red  $\rightarrow$  black at some fixed rate, and we thus posit the differential system:

$$\frac{dG}{dt} = -\beta FG, \tag{2.1}$$

$$\frac{dF}{dt} = \beta FG - \gamma F,$$

$$\frac{dB}{dt} = \gamma F.$$

Here,  $\beta$  is the ignition coupling constant, and the constant  $\gamma$  is the reciprocal of the burn-time of an  $F$  tree.

Before we continue with intuition and theory for this conflagration model, we observe the convenience that the classical susceptible( $S$ )-infected( $I$ )-recovered( $R$ ), or  $SIR$  epidemiological model dating back to [Kermack and McKendrick 1927] lies in 1-1 correspondence. In fact the assignments

$$G \rightarrow S, F \rightarrow I, B \rightarrow R$$

yields the fundamental  $SIR$  differential system. Incidentally, the identification of a burnt tree with a “recovered” tree is not so specious: There might be trees that, though “burnt”, remain alive. Moreover, in either the forest-fire scenario or an epidemic scenario, one may add differential equations and attendant parameters in order to quantify natural mortality. Note that in the above system we have not even included *natural* mortality such as a death-rate term for  $G$  trees, so this simplified fire model assumes a conflagration of much shorter time-scale than tree lifespan , and so on.

A typical time-evolution graph of  $F, G$  appears in Figure 1.

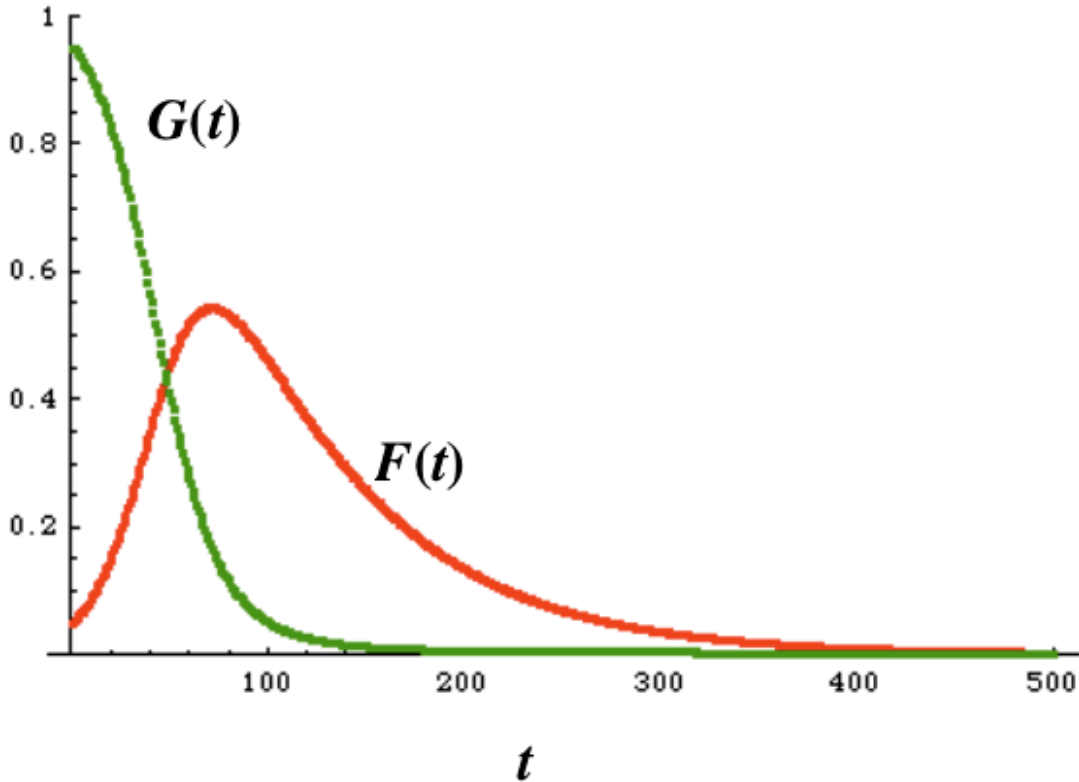


**Figure 1:** Typical time evolution for the  $GFB$  system (2.1). For a wide range of  $\beta, \gamma$  parameters, the total fire trees  $F(t)$  peaks out, then decays asymptotically to  $F(\infty) = 0$ . A first lesson of this simplified  $GFB$ —equivalently  $SIR$ —model is that the  $G(t)$  trajectory always has a positive asymptote  $G(\infty) > 0$  (albeit sometimes only slightly positive, as in the graph here). That is, as can be rigorously proved, *there are always survivors*.

The reason why we need not plot  $B$  trees in such as Figure 1 is that we have a conservation law:

$$\frac{d(F + G + B)}{dt} = 0,$$

as is evident immediately upon summing all three equations of the system (2.1). So the total count of trees  $F(t) + G(t) + B(t)$  is conserved and it is enough to analyze the  $F, G$  system only.

We now proceed to analyze the coupled  $F, G$  system of (2.1) theoretically. This is not merely an attractive exercise—it turns out that many of the analytic ideas translate into more sophisticated models such as a full-blown smallpox model. Everything that follows can be found in or inferred from analyses in the literature [11], although our manner of proof follows more in the spirit of typical mathematical-physics development. It is especially interesting—and good for the field of epidemiology—that this fundamental model, though a nonlinear system, can be solved; if not exactly in the time domain, at least exactly in its important aspects.

The first-order system (2.1) is completely driven by initial conditions, say  $F(0), G(0) > 0$  whence  $B(0) = (\text{constant}) - F(0) - G(0)$ . Formal integration of the  $dG/dt$ ,  $dF/dt$  equations yields:

$$\begin{aligned} G(t) &= G(0) e^{-\beta \int_0^t F(\tau) d\tau}, \\ F(t) &= F(0) e^{\int_0^t (\beta G(\tau) - \gamma) d\tau}. \end{aligned} \quad (2.2)$$

Now, happily, a phase-space ( $F$  vs.  $G$ ) trajectory can be obtained by dividing the first differential equation into the second, to obtain

$$\frac{dF}{dG} = -1 + \frac{\gamma}{\beta G},$$

whose exact solution is

$$F(t) = F(0) + G(0) - G(t) + \frac{\gamma}{\beta} \log \frac{G(t)}{G(0)}. \quad (2.3)$$

Another useful relation is obtained by cancelling the coupling term  $\beta FG$  in the (2.1) system:

$$\frac{dF}{dt} + \frac{dG}{dt} = -\gamma F,$$

so that

$$F(t) + G(t) = F(0) + G(0) - \gamma \int_0^t F(\tau) d\tau. \quad (2.4)$$

We may now derive some important, rigorous observations as follows (referring to the graph of Figure 1 is instructive), where time  $t \in [0, \infty)$ :

### Results for the *GFB (SIR) model*:

(2.5)

- Both  $F(t), G(t)$  are always positive, with  $G(t)$  monotone decreasing, as follow from (2.2).
- $F(t)$  is monotone decreasing iff  $G(0) < \gamma/\beta$ , from (2.2). Otherwise  $F(t)$  has one local maximum (as in Figure 1) where  $G(t)$  crosses  $\gamma/\beta$ , said maximum given then by (2.3).
- $F(t)$  is bounded (from (2.3)) and  $F$  is integrable (from (2.4)).
- $G(\infty) > 0$ , from (2.2) and the previous bullet; hence  $G$  is not integrable.
- $F(\infty) = 0$ , from (2.2) and previous bullet.
- The survivors' asymptote  $G(\infty)$  is thus given exactly (via (2.3)) by the solution to

$$G(\infty) - \frac{\gamma}{\beta} \log \frac{G(\infty)}{G(0)} = F(0) + G(0).$$

- The “total fire strength” (integrated  $F$ ) is given by

$$\int_0^\infty F(\tau) d\tau = \frac{1}{\gamma}(F(0) + G(0) - G(\infty)).$$

It is legendary that such a model (in equivalent  $SIR$  form) succeeded remarkably well in describing the 1905-1906 Bubonic Plague of New Delhi; there have since been explicit quantitative assignments of the key  $\beta, \gamma$  parameters to fit other epidemic data under such a model [1].

[ADD: The actual K–M sech relation model for the New Delhi plague.]

[ADD: Other success examples for the classical  $SIR$  model]

Note a key conclusion—the second bullet of the collection (2.5)—that an “epidemic threshold” is signalled by the relation  $G(0) > \gamma/\beta$ . When this inequality holds, the fire (infection) “takes off” with an initially positive slope, and an unfortunate peak in  $F$  is expected. A different way to see this effect is embodied in the last bullet of (2.5): Higher  $G(0)$  or lower  $\gamma$  generally causes greater total strength of the fire (infection).

To begin with such intuition on conflagration is not just pedagogically motivated. Indeed, there are ongoing studies of actual forest-fire quantification.

[ADD: References on forest-fire work.]

In the next section we shall extend these notions to a fundamental, still spatially-independent, smallpox model. It is to be stressed that the forest-fire picture is simply a symbolic expedient; later, we shall revisit the fire scenario for reasons of physical intuition.

### 3. Natural extension to a smallpox model

We shall now use the previous conflagration model to develop a spatially-independent model for smallpox *per se*, with other disease-outbreak models obtainable in similar fashion. We now revert to  $SIR$  symbology, though, for consistency with the epidemiological literature.

[ADD: Brief medical description of the stages of smallpox, and how these amount to a kind of “fire” that moves through various stages, as in a “smoldering” tree ( $I_1$ , say), a flaming tree  $I_2$ , say) and a tree near the end of its flameout...include, perhaps, something about how smallpox is dormant for some days, at first, etc.]

Our nomenclature involves various indices on time-dependent variables, which indices must be handled with care in any analysis. We assume two immune statuses (1 = normal, 2 = compromised immunity), three infectious states  $j = 1, 2, 3$ . Of special importance for

model generalization is a parameter  $c$  which denotes a “contact class” of susceptibles. For example, values of  $c$  can denote the type of family environment, the population density at the susceptible’s location, and so on. Leaving this class parameter  $c$  abstract for the moment, our nomenclature reads as follows:

$S_i(c, t)$  = susceptibles of immune status  $i \in 1, 2$ , and contact class  $c$ .

$I_{ij}(t)$  = infecteds of (original) immune status  $i \in 1, 2$ , and disease state  $j \in 1, 2, 3$ .

$R_i(t)$  = recovereds of (original) immune status  $i = 1, 2$ .

$\mu_i$  = natural (smallpox-unrelated) death rate by immune status  $i \in 1, 2$ .

$\Lambda_i(c, t)$  = infection rate for given immune status  $i \in 1, 2$ , and contact class  $c$ .

$\gamma_{i,j}$  = rate of disease progression for  $i \in 1, 2$ ,  $j \in 1, 2, 3$ .

$\delta_{i,j}$  = smallpox death rate for  $i \in 1, 2$ ,  $j \in 2, 3$ .

Note that  $\Lambda$  is a coupling matrix that determines all manner of infection processes, so that the dynamical character of the subsequent differential system depends strongly on the form of the  $\Lambda$  matrix. One arrives at the temporal-continuum equations by standard methods of rate-balancing (when  $(t)$ -dependence is obvious, we drop it for economy of notation, as in  $dI/dt = dI(t)/dt$ ):

$$\frac{dS_i(c, t)}{dt} = -\Lambda_i(c, t)S_i(c, t) - \mu_i S_i(c, t), \quad (3.1)$$

$$\frac{dI_{i1}}{dt} = \sum_c \Lambda_i(c, t)S_i(c, t) - (\mu_i + \gamma_{i1}) I_{i1},$$

$$\frac{dI_{i2}}{dt} = \gamma_{i1} I_{i1} - (\gamma_{i2} + \mu_i + \delta_{i2}) I_{i2},$$

$$\frac{dI_{i3}}{dt} = \gamma_{i2} I_{i2} - (\gamma_{i3} + \mu_i + \delta_{i3}) I_{i3},$$

$$\frac{dR_i}{dt} = \gamma_{i3} I_{i3} - \mu_i R_i.$$

As an important check on the integrity of this system, we observe by summing all left-hand sides that if we denote the total (living) population of type- $i$  immune status by

$$P_i = \sum_c S_i(c, t) + \sum_j I_{ij} + R_i,$$

then

$$\frac{dP_i}{dt} = -\mu_i P_i - \sum_{j=2}^3 \delta_{ij} I_{ij},$$

so that in absence of any death rates (simply pretend the “common cold” mode whereby death rates are all essentially zero on short-time scales) we have

$$\frac{d}{dt} (P_1 + P_2) = 0,$$

and thus total population is conserved. In this way the differential system obeys population conservation, modulo, of course, mortality effects. Such conservation laws are one of the surprisingly small set of features that discrete and continuum disease models do share—in any discrete model one should test integrity by turning off mortality momentarily, to verify that the (integer) population is invariant.

We have indicated that the coupling matrix  $\Lambda$  determines, in large measure, system behavior. One way to postulate the structure of  $\Lambda$  is to cast  $\Lambda_i(c, t)$  as a dot-product:

$$\Lambda_i(c, t) = \vec{\beta}_i(c) \cdot \vec{I}(t), \quad (3.2)$$

where  $\vec{I} = (I_{12}, I_{13}, I_{22}, I_{23})$  is a four-vector indicating the possible infectious sources to which the susceptibles are exposed, and the vector  $\vec{\beta}_i(c)$  involves any manner of combinatorics

that describe the infection rates. Thus, the vector, via the indicated dot-product, “infects” susceptibles according to the sum of rates, each rate arising from a separate  $I_{ij}$  with  $i \in 1, 2, j \in 2, 3$ . What is attractive about the dot-product decomposition is that transition to discrete models (and back, say) is made possible by interpreting  $\vec{\beta}_i(c)$  as a collection of stochastic terms, such as infection probabilities depending on immune status  $i$  and class  $c$ . Moreover, the transition to spatial dependence is made possible by allowing the class  $c$  to have a geographical component, as we shall see. In summary, we have described a temporal-continuum system and nomenclature that can be generalized into discrete, or spatial forms, or combinations of these extensions.

An interesting research avenue is as follows: What results of the type in collection (2.5) accrue for such a fundamental smallpox model? For example, assuming reasonable coupling constants in the smallpox model (3.1), what is the “epidemic threshold” (for which at least one of the  $I_{ij}$  has a local peak)? Are there always “never infecteds” ( $S_i(c, \infty) > 0$ )? The hope is that the formal-integration and phase-space methods would be enough to answer such theoretical questions.

#### 4. Simple spatial-dependent fire model

We have spoken of time-dependent conflagration (infection) with integration over the spatial dimensions implicit. It is perhaps best to introduce spatial dependence in a discrete, heuristic style, in the spirit of the standard physics development of differential systems via microscopic transition probabilities.

Say that lattice points in an  $(x, y)$ -planar “forest” of lattice-cell dimensions  $\delta \times \delta$  have probabilities  $g(x, y, t)$ ,  $r(x, y, t)$ ,  $b(x, y, t)$  of being “green, on-fire, burnt” respectively. We demand  $g + r + b = 1$  for all space and time, and posit relations involving a small time quantum  $\tau$ :

$$f(x, y, t + \tau) = f(x, y, t)(1 - \gamma\tau) + \frac{\beta\tau}{4}g(x, y, t)(f(x + \delta, y, t) + f(x - \delta, y, t) + f(x, y + \delta, t) + f(x, y - \delta, t)), \quad (4.1)$$

and

$$g(x, y, t + \tau) = g(x, y, t)\left(1 - \frac{\beta\tau}{4}(f(x + \delta, y, t) + f(x - \delta, y, t) + f(x, y + \delta, t) + f(x, y - \delta, t))\right). \quad (4.2)$$

Here,  $\beta, \gamma$  are ignition-coupling constant and fire-decay rate, respectively (so that the mean time to extinguish is  $T = 1/\gamma$ ). (The  $1/4$  factor is a convenience, for comparisons to other models.) We are envisioning the fire “jumping” each of north/east/west/south directions with probability  $\beta\tau$ , and that fire trees do decay into black trees at a rate  $\gamma$  per unit time. Figure 2 shows a schematic of the possibilities.

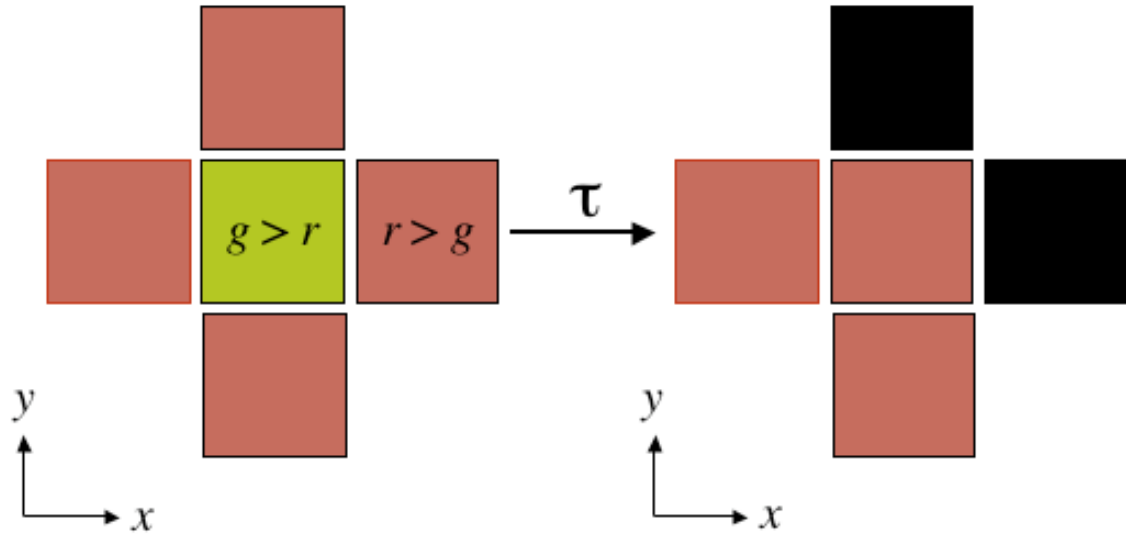


**Figure 2:** A typical discrete fire scenario for the system (4.1), (4.2). A high- $g$  value (center “green” location can become an ( $r > g$ ) location (at right) with some fire locations also burning out (to  $b > f$ ). This “discrete-analog” approach involves, say, real-valued  $f, g, b$ , whereas qualitatively similar overall behavior is afforded by simply transitioning between only three possible colors (see text and Figure 3).

Before we move to analysis of the system (4.1), (4.2), we observe that computer programs that approximate the system by forcing every  $(x, y)$  location to be *only* one of (*green, red, black*) tend to show qualitative similarity to the probability evolution. That is, if we do not “shade” each tree according to probabilities  $(g, r, b)$ , instead simply allowing fire to jump with probability  $\beta\tau$  from red to green trees, we obtain scenarios exemplified in Figure 3.

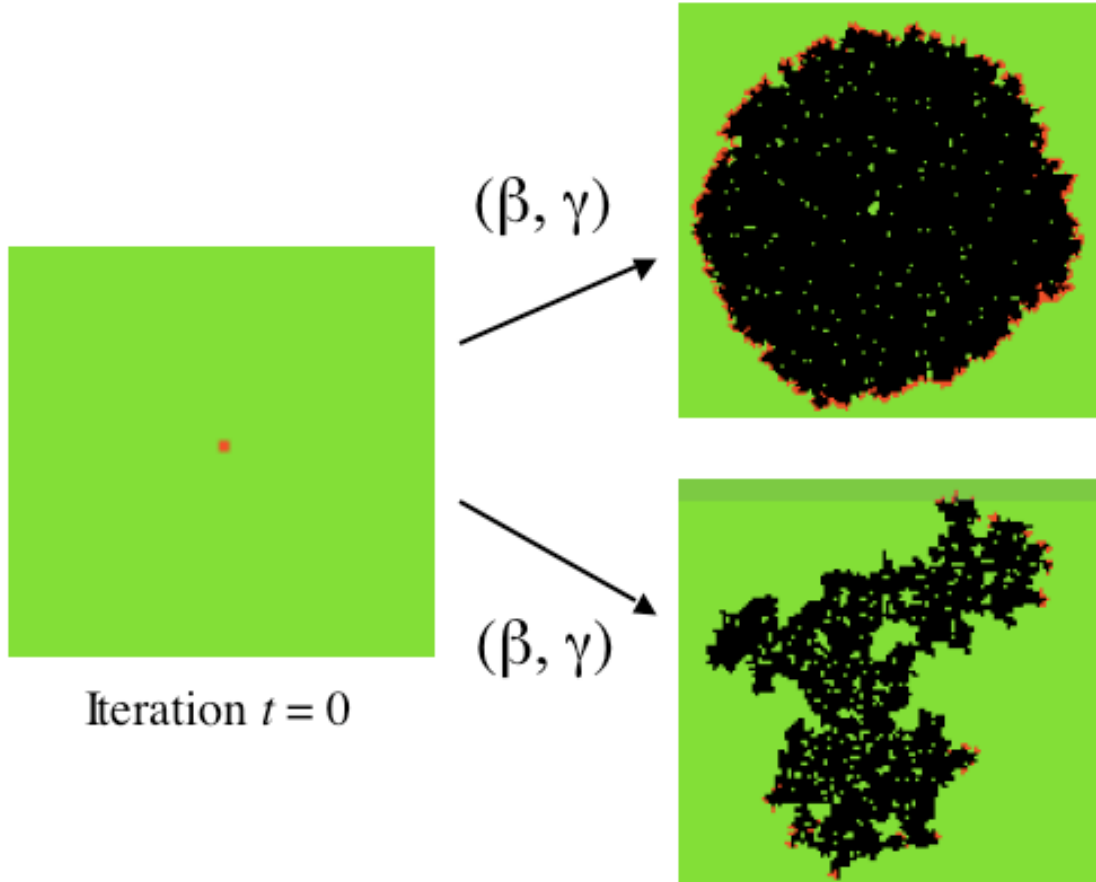
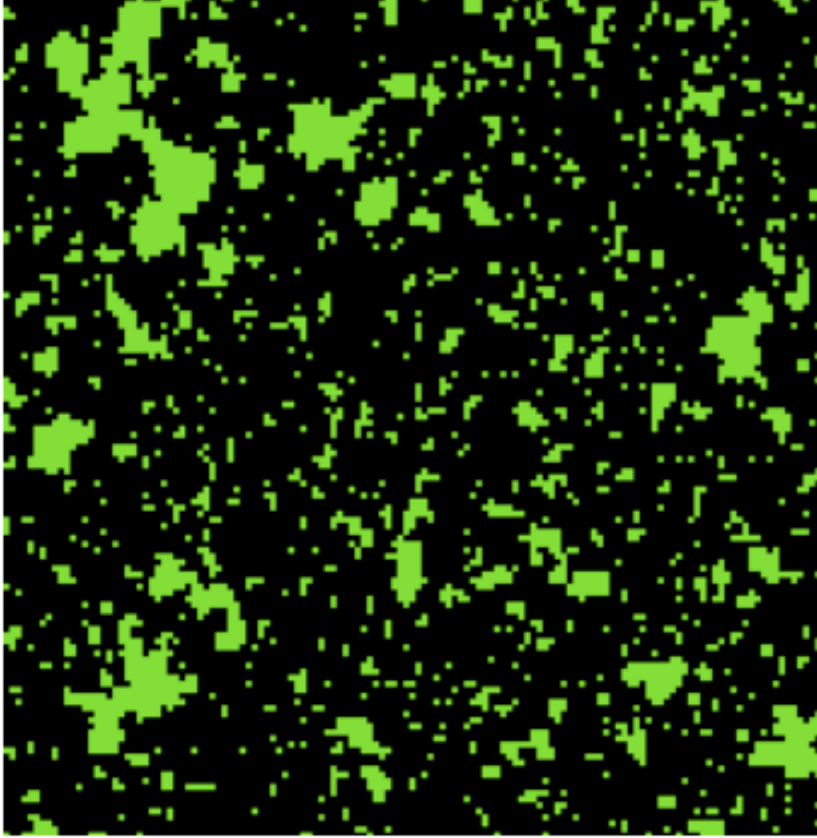


**Figure 3:** If the discrete-conflagration system (4.1), (4.2) is further reduced so that a tree’s triple  $(g, r, b)$  is always a permutation of  $(1, 0, 0)$ , with such tertiary transitions still governed in an obvious sense by  $(\beta, \gamma)$ , then we can obtain via computer model either a radially progressing fire-front (upper right), or, with different  $(\beta, \gamma)$  parameters, peculiar fire epidemics of a qualitatively different character (lower right). Though we later describe epizootic wavefronts with attendant propagation velocities in the continuum picture, it is difficult for obvious reasons to be precise about such as a “wavefront” in a discrete model.

The parameter domain for which the conflagration leaves a substantial survivor  $(g(x, y, \infty) > 0)$  set is especially interesting. Figure 4 shows a typical result for certain parameters, with survivor (green) set having statistical-fractal character.



$$\delta \sim 1.72$$

**Figure 4:** For certain parameters  $(\beta, \gamma)$  in the tertiary epidemic model ((4.1), (4.2) system interpreted for  $(g, r, b)$  being permutations on  $(1, 0, 0)$ ) leaves a “fractal” survivor set. For the experimental run shown, the measured fractal dimension (quantified in separate research) is 1.72; i.e., the  $\{g(x, y, \infty)\}$  set is “more than a (1-dim) line” and “less than a (2-dim) plane.”

The fractal survivor-set notion is amplified in a separate treatment [?, ?, ] where implications for vaccination strategies (based on such dimension  $\delta$ ) abound. For the moment we merely observe that such discrete models give rise qualitatively distinct to phenomena as compared to continuum models.

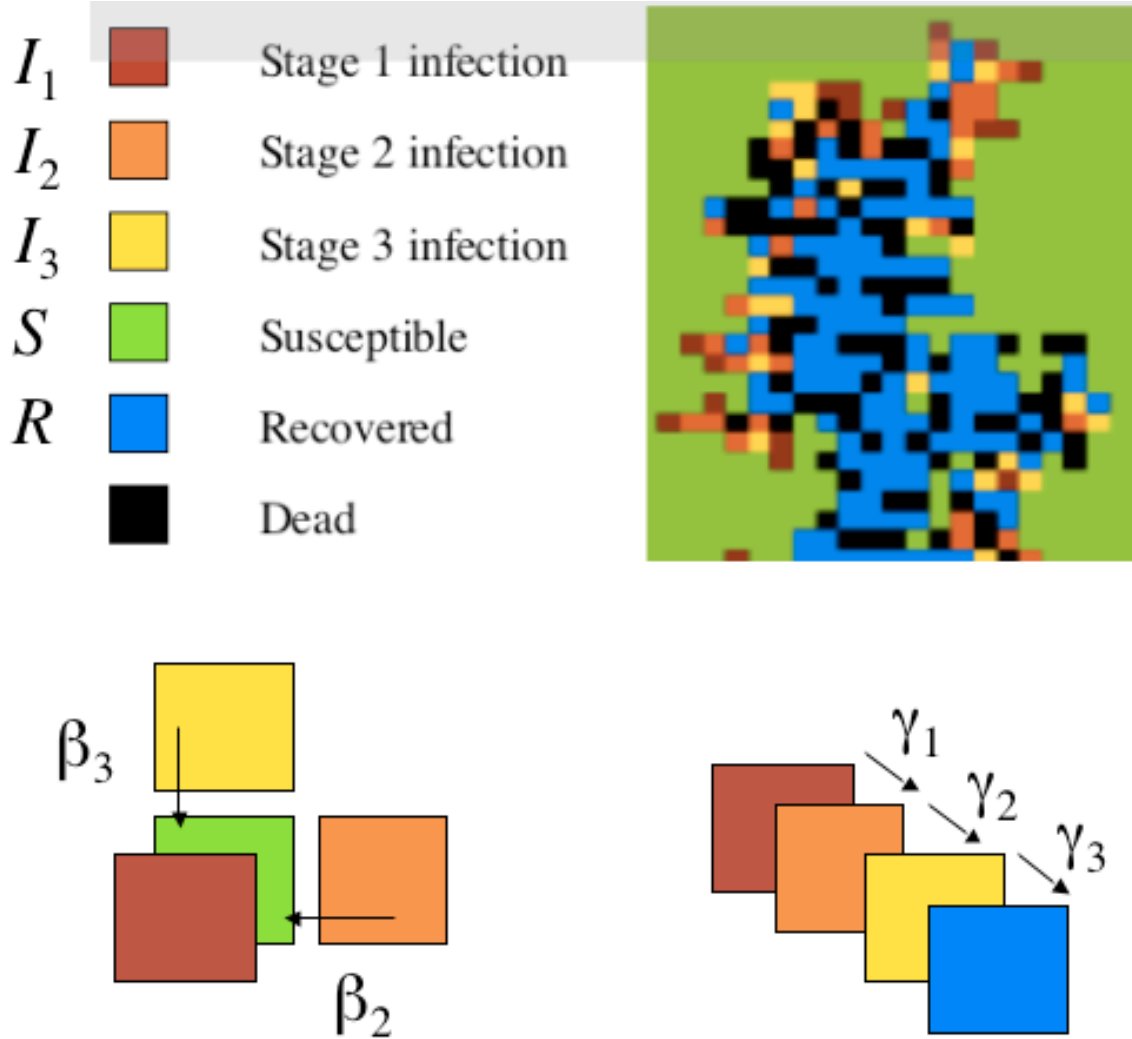


**Figure 5:** Typical appearance of a smallpox-relevant extension to the model (4.1), (4.2) with states being permutations on  $(1, 0, 0, 0, 0, 0)$  of susceptible, (three) infected, recovered and dead possibilities. (See text for descriptions of the  $(\beta, \gamma)$  nonlinear-coupling algebra.) At upper right is a typical epidemic result starting from a smallpox attack analogous to the initial  $(t = 0)$  forest-fire state of Figure 3. Again we obtain complicated, perhaps fractal densities of survivors (green or blue), as would be difficult if not impossible to infer from continuum theory.

In Figure 5, the lower-left pictorial means that a green ( $S$ ) element is changed to a red ( $I_1$ ) based on discretization of the first equation in smallpox system (3.1), with the  $\Lambda$  product (3.2) given by

$$\Lambda = \vec{\beta} \cdot \vec{I} = (\beta_2, \beta_3) \cdot (I_2, I_3) = \beta_2 I_2 + \beta_3 I_3,$$

where we are ignoring for this discrete picture the immune status, contact class, and zeroing the mortality terms. Thus for one time step (say  $\tau = 1$ ) we have a transition probability

$$prob(S \rightarrow I_1) = \beta_2 \#\{I_2 \text{ neighbors}\} + \beta_3 \#\{I_3 \text{ neighbors}\}.$$

Thus, simple counting of the # of neighboring elements of respective color suffices. The lower-right pictorial does not involve any neighbors, instead for  $k = 1, 2$  we adopt:

$$prob(I_k \rightarrow I_{k+1}) = \gamma_k$$

and

$$prob(I_3 \rightarrow R) = \gamma_3.$$

So, in the spirit of system (4.1), (4.2) we force each element to be one of five colors instead of keeping analog (continuous) values of everything at each element.

Now, back to the iterative system (4.1), (4.2). It is a classical expedient in stochastic approximations to involve the Laplacian operator  $\nabla^2$  via:

$$f(x + \delta, y, t) + f(x - \delta, y, t) + f(x, y + \delta, t) + f(x, y - \delta, t) \approx 4f(x, y, t) + \delta^2 \nabla^2 f \quad (4.3)$$

and

$$f(x, y, t + \tau) - f(x, y, t) \approx \tau \frac{\partial f}{\partial t}.$$

Then the associated differential system is:

$$\frac{\partial g}{\partial t} = -\frac{1}{4}\beta\delta^2 g \nabla^2 f - \beta f g, \quad (4.4)$$

$$\frac{\partial f}{\partial t} = \frac{1}{4}\beta\delta^2 g \nabla^2 f + \beta f g - \gamma f.$$

This system compares interestingly with the spatially independent system (2.1) for the *GFB* (equivalently, *SIR*) model. A fundamental observation here is that even though “trees do not move”, the notion of fire-jumping leads to Laplacian terms, and hence to spatial dependence. Incidentally, the peculiar (−) sign of the Laplacian term in the first equation of (4.4), and also the lack of a positive Laplacian term for green trees is just what we admitted: Trees do not move. When we turn to a space-time smallpox model, there will be indeed Laplacian terms attendant on the spatial mobility of susceptibles.

Instead of analyzing the interesting system (4.4), we next move to an analysis of what might be called a canonical space-time system, with a view to actual space-time disease propagation.

## 5. 2-dimensional space-time continuum fire model

Even though “trees do not move” we have seen that spatial terms can arise from intuitive microscopic rules.. Before we address the issue of moving organisms, let us analyze a conflagration model where  $g(x, y, t)$ ,  $f(x, y, t)$ ,  $b(x, y, t)$  satisfy:

$$\frac{\partial g}{\partial t} = -\beta f g, \quad (5.1)$$

$$\begin{aligned}\frac{\partial f}{\partial t} &= D\nabla^2 f + \beta fg - \gamma f, \\ \frac{\partial b}{\partial t} &= \gamma f.\end{aligned}$$

This system differs from the classical one (2.1) only in the introduction of the Laplacian term. We admit that we have not posited a microscopic model for (5.1)—compare system (4.4)—however such a microscopic foundation can be effected via suitable modification of the microscopic fire-jumping rules.

First, in the theoretical-physics spirit, we note a conservation law that holds for suitably behaved  $f$ . using integrals over all space vectors  $\vec{r}$  we write:

$$\frac{\partial}{\partial t} \int (g + f + b) d^2\vec{r} = \int \nabla^2 f d^2\vec{r} = 0.$$

Here, the second space integral vanishes by the often invoked Green’s theorem, that said integral is the limit of a very large flux integral, so that for a very wide class of  $f$  solutions (say,  $f$  is damped exponentially as  $|\vec{r}| \rightarrow \infty$ ) this integral vanishes. We then have the full space integral of  $g + f + b$  being constant in time. And here is another reason to introduce (Laplacian) spatial terms into any epidemic model: Conservation laws are usually immediate.

Note the diffusion constant  $D$  in system (5.1), in the sense that free diffusion of some density  $p$  in simple, linear, classical settings takes the form

$$\frac{\partial p}{\partial t} = D\nabla^2 p, \tag{5.2}$$

whose impulse solution is known exactly:

$$p(x, y, t) = \frac{1}{4\pi Dt} e^{-(x^2+y^2)/(4Dt)}.$$

Now this impulse solution implies that free diffusion *always* causes a “melting” or “spreading” of any initial density  $p(x, y, 0)$ . However, it is a fascinating and telling fact that the nonlinear terms of (5.1) can “shore up” a wavefront, allowing stable waves (reminiscent of “solitary” waves, or in special instances “solitons” of physics origin) to propagate with an asymptotically fixed velocity.

Figure 6 shows typical such solitary waves in pictorial fashion. In the equivalent epidemiological setting these are called epizootic waves [1].

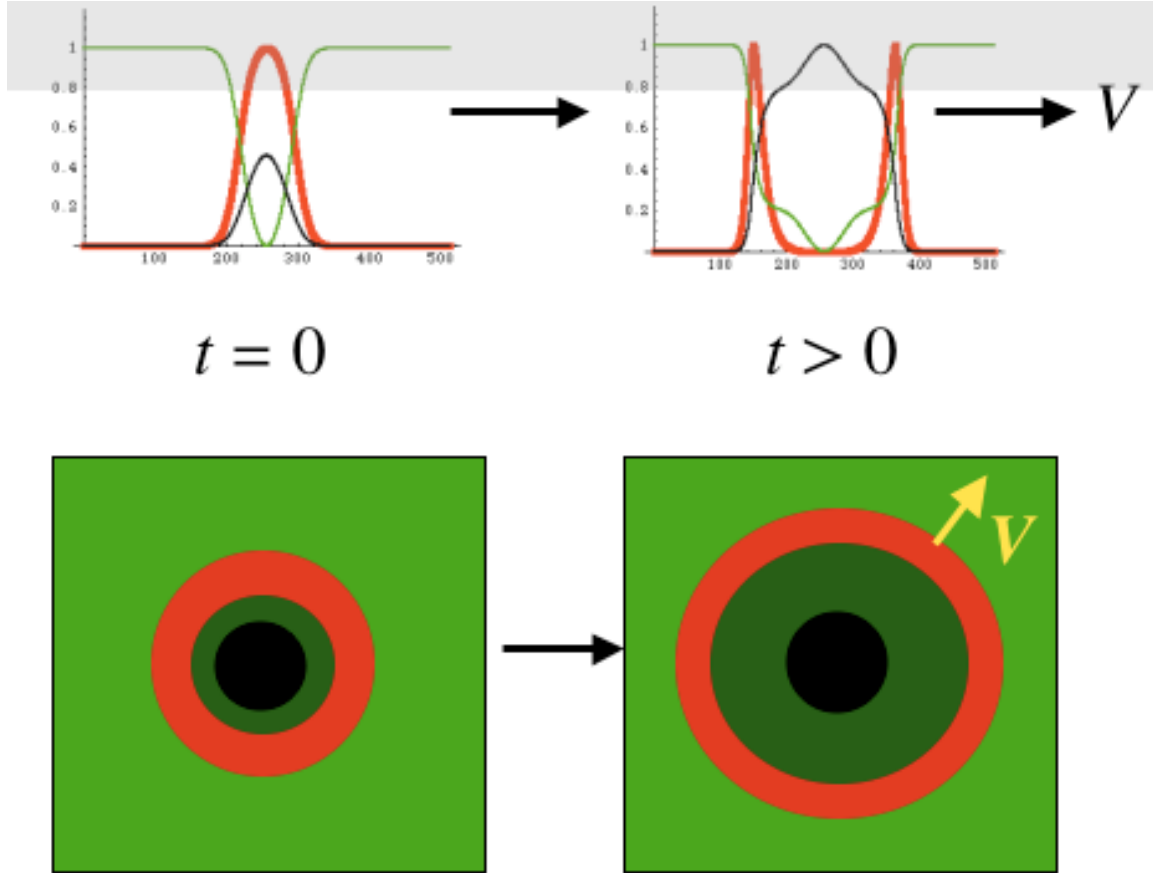


**Figure 6:** 1- and 2-dimensional propagation for the space-time system (5.1). In 1-dimensional formalism—depending on  $(D, \beta, \gamma)$  parameters—one obtains outgoing pulses of conflagration, with a speed  $V$  that can be analytically bounded (top of figure). In (5.1), the diffusion ( $D$ -factor) spreading term is essentially overcome via the nonlinearity. In 2-dimensional scenarios, one again obtains an outgoing velocity—the bottom of the figure just shows a caricature of computer solutions. Qualitative similarity of the (lower-right) circular pictorial here with the upper-right of Figure 3 is instructive.

Incidentally, a good precedent for system (5.1) is the fox-rabies model of [], whereby rabid foxes “diffuse” on an assumption of infected-organisms (signified by density  $f$ ) meandering rather randomly across the  $(x, y)$  plane. In fact, the system (5.1) is formally equivalent (in the 1-dimensional setting) to [?]. The beautiful analysis of that reference can be summarized as follows. Assume an asymptotic solitary wave (upper right of Figure 6), with velocity  $V$  in the sense:

$$g(x, t) \sim G(x - Vt), \quad f(x, t) \sim F(x - Vt).$$

The system (5.1) then reads, in the 1-dimensional setting,

$$VG' \sim \beta FG,$$

$$DF'' + VF' + F(\beta G - \gamma) \sim 0.$$

If we assume  $G(z) \sim_{z \rightarrow \infty} 1$  as in the upper right of Figure 6, then we expect

$$F(z) \sim A e^{\left(-V \pm \sqrt{V^2 - 4D(\beta - \gamma)}\right)/(2D)}.$$

But the positive-definite  $F$  cannot oscillate, so we have a condition

$$V_{\min} = \sqrt{4D(\beta - \gamma)}.$$

Computer studies indicate that this  $V_{\min}$  is the asymptotic velocity, although we authors know of no rigorous results in this direction. (Eigenvalue studies and critical-point physics certainly suggest, though, such an asymptotic velocity.) Remarkably—even though the system is patently nonlinear—we may also determine the survivor limit, from

$$DF'' + VF' + \frac{VG'}{\beta G}(\beta G - \gamma) = 0,$$

whose integrated form implies that

$$G(0) - \frac{\gamma}{\beta} \log G(0) = 1.$$

The solution  $G(0)$  to this transcendental relation compares well computationally with asymptotic survivor results for the simple spatially independent model (2.1). This  $G(0)$  is the asymptotic density of the (green) survivor curve (about 0.2 at the horizontal axis in the upper right of Figure 6).

For epizootic waves in 2 dimensions, we start with system (5.1) and assume the remote (large- $r$ ) regions have  $g(x, y, t) \sim 1$ . This scenario affords us the opportunity to borrow yet another expedient of physics. Namely, the second of (5.1) when written

$$\frac{\partial f}{\partial t} \sim D \nabla^2 f + (\beta - \gamma)f \tag{5.3}$$

suggests a (radial) solution

$$f(r, t) \sim \frac{1}{t} e^{(r^2 - 4D(\beta - \gamma)t^2)/(4Dt)}.$$

Actually, this solution is exact if (5.3) be deemed an equality. Now if  $r \approx Vt$  where the velocity  $V = \sqrt{4D(\beta - \gamma)}$ , then a further approximation is

$$f(r, t) \sim \frac{1}{t} e^{-V(r - Vt)/(2D)}. \tag{5.4}$$

This is a spatially exponentially damped wave—the “tail” of the conflagration extending beyond  $r = Vt$ , and this tail moves with speed  $V$ . Heuristically, then, we expect the  $f$  pulse itself to move with radial speed  $V$ . Without more rigor it is not clear how the *amplitude* of said epizootic wave’s peak changes with large times  $t$ , but at least we can derive that

(5.4) correctly solves (5.3) to order  $1/r$ . Note that for such analyses the 2-dimensional radial Laplacian operator is  $\nabla^2 = d^2/dr^2 + (1/r)d/dr$ .

Such analysis gives the same heuristic epizootic velocity  $V = \sqrt{4D(\beta - \gamma)}$  as for the 1-dimensional case. This is not unreasonable, since after all, at great distances (large  $r$ ) the wavefront has vanishing curvature.

The above techniques all fall under a general rubric: so-called “linearization” of the nonlinear system about stable dynamical points, such as  $(f, g, b) \sim (1, 0, 0)$  for large  $r - Vt$ . An interesting approach to enhanced rigor would be to search for symbolic series that resolve the system (5.1). Such methods have been known to provide extreme position in other nonlinear studies [ ].

## 6. Microscopic contact dynamics

We have seen at multiple junctures that a “contact rate” (or, in physics terms, a nonlinear coupling constant)  $\beta$  is ubiquitous. In such as the smallpox contact dot-product construct  $\Lambda$  in (3.2), we ask: What precisely is the contact rate (the vector  $\vec{\beta}$ )? Moreover, we would like to connect this question with the spatial-dependence formalisms previous.

One way to proceed on this contact-rate issue is to adopt a “hard-disk” model, whereby susceptible ( $S$ ) disks and infected ( $I$ ) disks each diffuse under classical diffusion, with respective diffusion constants  $D_S, D_I$ . Note we are avoiding a conflagration model in the sense that now every organism *moves*. Figure 7 shows the basic idea.

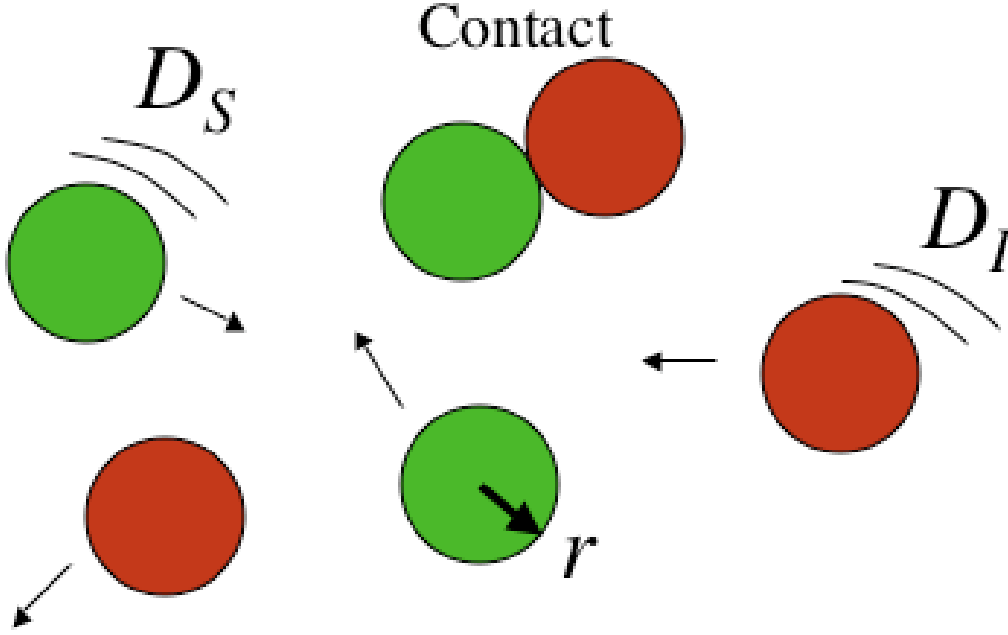


**Figure 7:** A disk-collision model, with effective contact radius  $r$ , whereby susceptible (green) disks and infected (red) disks meander with respective diffusion constants  $D_S, D_I$ . The contact rate depends in a complicated way on  $D_S, D_I, r$  and the characteristic time quantum  $\tau$ .

If we imagine the disks in Figure 7 to achieve their respective diffusion constants via microscopic meandering, with a typical classical estimate

$$D \approx \frac{\sigma^2}{2\tau},$$

where  $\sigma^2$  is the short-time spatial-motion variance, for short times  $\tau$ —as leads to the classical equation (5.2)—we obtain, after intricate analysis as pertains to molecular collision dynamics, to an effective rate:

$$\beta \approx \frac{cr}{\sqrt{\tau}} \sqrt{D_S + D_I}, \quad (6.1)$$

where  $c$  is an effective constant ( $\sim 1$ , depending on all dynamical assumptions). One way to start on such an intricate heuristic path is to observe that the total random-walk path-length  $L(T)$  after duration  $T$  due to relative velocities of the  $S, I$  species under the microscopic assumptions behaves as

$$\langle L(T) \rangle = T \sqrt{\frac{\pi}{\tau}} \sqrt{D_S + D_I},$$

and this is how various  $\sqrt{\quad}$  factors arise. Note that  $c$  should, realistically, also embody assumptions about infection probability *per contact*, and so on. Now, the physical dimensions

of  $\beta$  are space<sup>2</sup>/time, as befits a parameter such that  $\beta IS$  has the correct dimension (of say  $\partial S/\partial t$ , when  $S, I$  are densities of dimension 1/space<sup>2</sup>).

A caution is appropriate here. In the theory of molecular collisions, the diffusion constants depend on collisions themselves. We are *not* assuming this. Instead, our disks have diffusion constants resulting from, shall we say, locomotion. That is, our disks do not achieve random motion vis collisions; we are assuming random motion and estimating subsequent collisions between  $S, I$  species.

A physical example is appropriate here. Imagine  $S, I$  individuals at a gathering, a festival, with essentially random motions overall. If everyone stands still ( $D_S, D_I \approx 0$ ), contact is minimal. If, however, an infected  $I$  individual meanders rapidly (in the sense of  $\delta/\tau$  being large in the microscopic picture), then many  $S$  individuals will experience infective contact. If on the other hand, an  $S$  individual meanders rapidly, there is likewise more contact. The factor  $\sqrt{D_S + D_I}$  is thus bimonotonic—increasing in either diffusion parameter. The square-root occurs basically because mean-square velocities add in quadrature.

These rather heuristic observations lead to an interesting differential system:

$$\begin{aligned}\frac{\partial S}{\partial t} &= D_S \nabla^2 S - \lambda \left( \sqrt{D_S + D_I} \right) SI, \\ \frac{\partial I}{\partial t} &= D_I \nabla^2 I - \left( \lambda \sqrt{D_S + D_I} \right) SI - \gamma I.\end{aligned}\tag{6.2}$$

Here, the constant  $\lambda$  is intended to incorporate infection probability per contact, the effective radius  $r$  of infectious contact, and so on. In other words,  $\lambda$  is assumed proportional to the  $\beta$  of (6.1). In the event that diffusion parameters are *themselves* spatially dependent, one may invoke reaction-diffusion theory [] to assign:

$$D \frac{\partial^2}{\partial x^2} \rightarrow \frac{\partial}{\partial x} D(x) \frac{\partial}{\partial x},\tag{6.3}$$

with appropriate, standard generalization to  $> 1$  dimensions.

Albeit heuristic and assumption-heavy, this analysis of contact rates does imply:

- The effective contact rate (6.1) is linear in “contact radius”, which could be a disease-dependent parameter (e.g., direct physical-contact transmission, airborne infection).
- The rate is increasing with (either of)  $D_S, D_I$  increasing; thus, mobility of either susceptibles or infecteds has an evident quantitative effect. Read: More motility on the part of either  $S$  or  $I$  organisms increases the contact rate.
- The time-scale of infection is important for the contact rate: Based on (6.1), it is not enough just to know the diffusion-related mobility; the characteristic time-step  $\tau$  also enters. Perhaps the best modeling approach is to simply adopt phenomenological parameters  $D_S, D_I$  in system (6.2) and proceed to develop global implications.

- If the effective organism mobility is a consequence of behavioral or geographical phenomena, then the complication of spatially (or even time-) dependent  $D$  values as in (6.3) should be observed.

## 7. Space-time smallpox model

Based on Section 3, and the previous sections on diffusion and contact rates, a possible space-time smallpox system runs as follows:

$$\frac{\partial S_i(c, t)}{\partial t} = D \nabla^2 S_i(c, t) - \Lambda_i(c, t) S_i(c, t) - \mu_i S_i(c, t), \quad (7.1)$$

$$\frac{\partial I_{i1}}{\partial t} = D \nabla^2 I_{i1} + \sum_c \Lambda_i(c, t) S_i(c, t) - (\mu_i + \gamma_{i1}) I_{i1},$$

$$\frac{\partial I_{i2}}{\partial t} = D_2 \nabla^2 I_{i2} + \gamma_{i1} I_{i1} - (\gamma_{i2} + \mu_i + \delta_{i2}) I_{i2},$$

$$\frac{\partial I_{i3}}{\partial t} = D_3 \nabla^2 I_{i3} + \gamma_{i2} I_{i2} - (\gamma_{i3} + \mu_i + \delta_{i3}) I_{i3},$$

$$\frac{\partial R_i}{\partial t} = D \nabla^2 R_i + \gamma_{i3} I_{i3} - \mu_i R_i.$$

Here we have simply shown for pedagogical purposes how *differing* diffusion constants may enter such a complex model. We have arbitrarily given  $S, I_{i1}, R$  populations the *same* diffusion constant, on the idea that other disease states physically involve different spatial-diffusion parameters (due to, say, impaired mobility or intentional/natural quarantine). We are quite aware that a great many other considerations are appropriate, such as neighborhood factors, population drifting of a nondiffusive nature, and so on. (The next section deals quantitatively with one of such side issues.)

Note that, per Section 6 on contact dynamics, the  $\Lambda$  constructs as in relation (3.2) in our space-time model (7.1) should rightfully involve  $\beta$  vectors which in turn depend on diffusion parameters  $D_i$ , as in our foray of Section 6. We do not write out such relations; instead we urge that a comprehensive theory that includes diffusion-mobility in the form of  $D \nabla^2$  terms should also involve  $D$  parameters in the contact algebra.

Incidentally, a researcher who wishes to model computationally the complicated space-time smallpox model (7.1) in the spirit of system (4.1)-(4.2) and Figure 5 can proceed as follows. Using the discrete-Laplacian relation (4.3), and the subsequent discrete time derivative, set up (7.1) as a lattice iteration. That much is conceptually simple. What is harder is to so

infer from sheer computation such phenomena as we have heretofore seen; namely, survivor set geometry, epizootic waves, and many other aspects.

## 8. Periodic-commuter theory

We would be remiss in not analyzing at least one scenario where organisms move in some methodical way, as opposed to sheer diffusive motion as discussed in Section 6. Other researchers have gone a great distance in handling human geography and demographics with respect to human behavior during epidemics [], and of course all of this is important in any realistic epidemic model.

What we shall do here is provide some epidemiological implications in regard to behavioral, “commuter” algebra. Namely, we shall assume that the population (of both  $S, I$ ) organisms follows a deterministic density fluctuation. The classical diffusion relation (5.2) becomes, when particles are modeled to drift with convection velocity  $\vec{v}$  (perhaps spatially dependent but time-independent) the following:

$$\frac{\partial p}{\partial t} = D\nabla^2 p - \nabla \cdot (\vec{v}p). \quad (8.1)$$

The beauty of such convection analysis in regard to epidemiology is that the obvious substitution of the Laplacian term by the convection-modified term is thus suggested.

In 1 dimension, when velocity  $v$  is constant, the kernel solution to (8.1) is

$$p(x, t) = \frac{1}{\sqrt{4\pi Dt}} e^{-(x-vt)^2/(4Dt)},$$

which is a spreading Gaussian packet whose peak moves with velocity  $v$ . However, as seen in many fields and in some of our previous analysis, *nonlinear* terms can overcome the temporal spreading. Consider a 1-dimensional commuter model (with, for the moment, no disease) governed by

$$\frac{\partial p}{\partial t} = D \frac{\partial^2 p}{\partial x^2} + \frac{\partial}{\partial x} (V \text{sign}(x)p). \quad (8.2)$$

Here,  $V > 0$  is a constant velocity but which, due to the  $\text{sign}()$  function, implies that organisms from either side of the  $x$ -axis move toward the origin. That is, organisms move toward a center ( $x = 0$ ) from either direction, as if they are going to a common center (as in, “going downtown in the morning”). Remarkably, (8.2) has a steady-state (time-independent) normalized solution

$$p = P(x) = \frac{V}{2D} e^{-V|x|/D}, \quad (8.3)$$

which is an exponential cusp centered at the origin. In effect: The convection overcomes the diffusive effect. Such a result is known in the form of insect-migration dynamics [] but we can say more. An exact solution to (8.2) can be given—for any initial conditions—in terms of Green functions [] from quantum physics (notably, for so-called delta-function potentials). Second, we may actually estimate the infective effect of *periodic* commuter motion.

Referring to Figure 8, note that an initially spatially uniform population evolves into the cusp (8.3) after a time of order  $T \sim L/V$ .

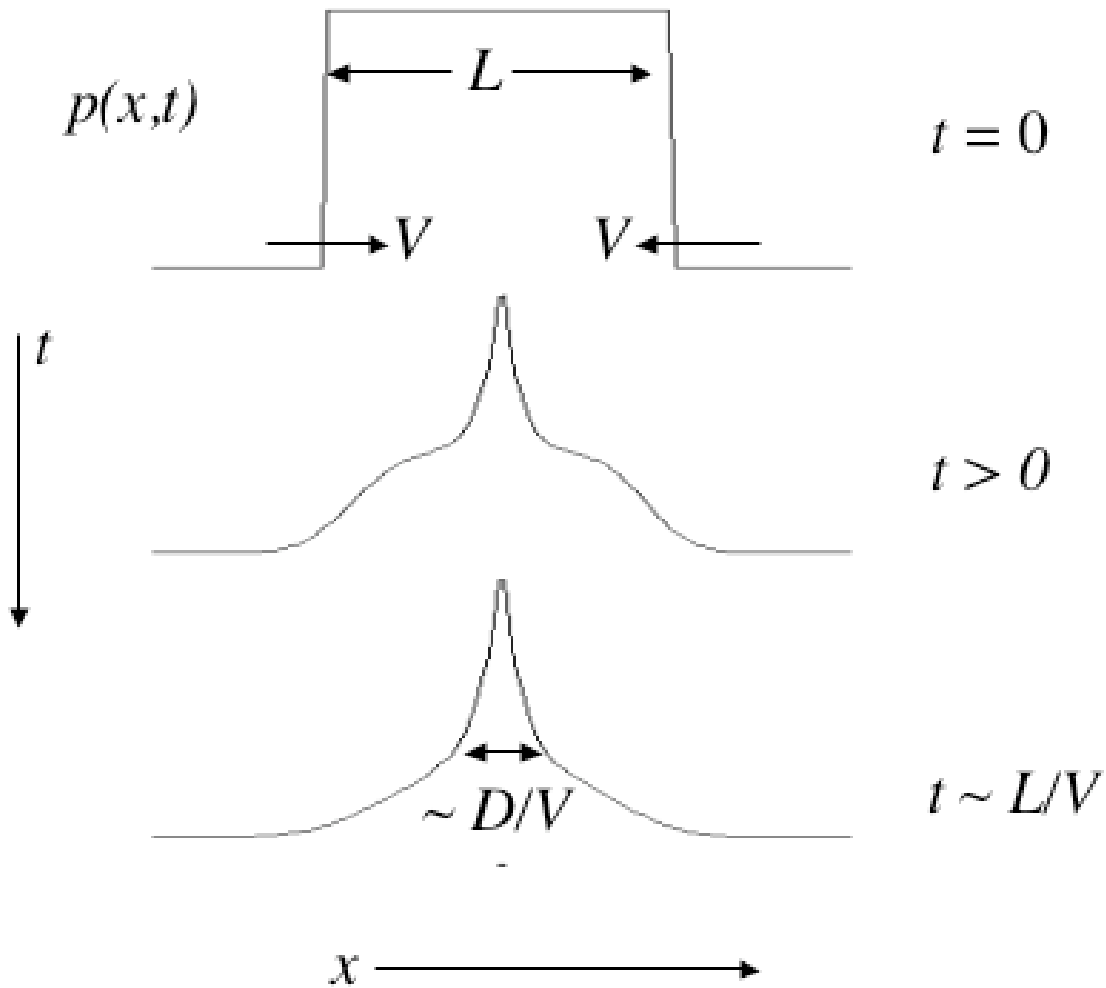


**Figure 8:** An initially uniform width- $L$  distribution in 1 dimension of organisms, who convect toward the “commuter” origin according to the differential equation (8.2) take a time about  $L/V$  to reach a stable cusp solution (8.3). (As if: The organisms “go to morning work.”) The asymptotically stable exponential-cusp solution has characteristic width  $D/V$ . This means that commuter dynamics—through parameters  $D, V$ —increases the effect of nonlinear infection coupling in a quantifiable way.

On the basis of such theory we can give an “infection gain” in the presence of such convective commuting. Heuristically, if the spatial span of the pre-commuting population is  $L$  (the width of the initial distribution atop Figure 8) then, by integrating the *square* of (8.3), on the idea that both  $S, I$  populations do commute toward the origin with infection rate being quadratic,

we have a dimensionless factor

$$\mathcal{I} \sim \frac{VL}{4D}.$$

which, when large, indicates an unfortunate gain in nonlinear infection terms. Simply put: The circadian “compaction” of populations can be expected to give rise to a roughly quantifiable infection gain. Of course, one might also insert a “duty-cycle” factor in the  $\mathcal{I}$  relation, for example a multiplier that embodies the fact of work-congregation happens only a fraction of the a 24-hour circadian cycle.

Such conclusions exemplify the occasional power of the continuum approach. It would be difficult to achieve such as the  $\mathcal{I}$  measure computationally. Albeit crude and simplified, this heuristic  $\mathcal{I}$  measure suggests that all three of  $L$  (pre-commute spatial span),  $v$  (commute-drift velocity), and  $D$  (a measure of organism motility) do figure in.

An interesting research avenue is to investigate long-term periodic solutions (say, with 24-hour period) to the convective system (8.2), and furthermore to do this for 2-dimensional space. (The population would converge with convective velocity  $\vec{v}$  aimed toward the spatial origin.)

Also interesting is that important scales shift when we move to a more realistic 2-dimensional model. The relevant diffusion variant is

$$\frac{\partial p}{\partial t} = D\nabla^2 p + V\nabla \cdot (p\hat{r}),$$

where  $\hat{r}$  is the unit radial vector. For constant velocity  $V$  (again all organisms commute toward the origin) the steady-state radial solution satisfies ( $p' = dp/dr$ ):

$$0 = D(p'' + (D/r)p') + Vp' + (V/r)p.$$

Interestingly enough, we again have an exponential cusp solution, normalized as

$$p(r) = \frac{V^2}{2\pi D^2} e^{-V|r|/D}.$$

Figure 9 shows an initially uniform population spread over a disk of diameter  $L$ , evolving in (roughly) time  $L/V$  to a stable “at work” cusp.

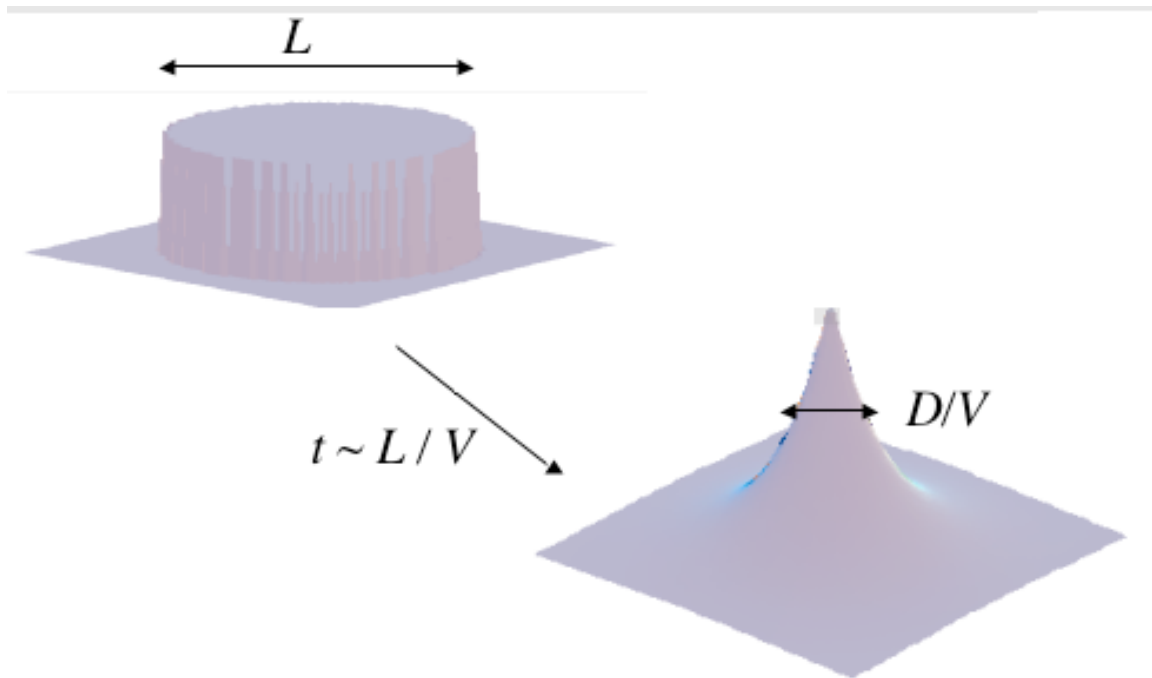


**Figure 9:** An initially uniform diameter- $L$  population disk commutes toward the origin in time  $L/V$  to a stale cusp distribution whose characteristic width is again  $D/V$ . However, the fact of 2 dimensions gives a much more unfortunate “infection gain”  $\mathcal{I}$ .

In the same way as the  $\mathcal{I}$  gain was derived for the 1-dimensional case, we assume that both  $S, I$  organisms have the initial disk distribution of Figure 9. Then integration over space of the quadratic term  $IS$  gives an infection gain

$$\mathcal{I} = \frac{V^2 L^2}{32D^2},$$

which is *far* worse than the 1-dimensional result. In fact, this 2-dimensional  $\mathcal{I}$  is essentially the *square* of the 1-dimensional value.

Such simplified analyses reveal the importance of behavioral phenomena, not to mention the issue of quarantine—i.e., preventing in one way or another the tight visitation of organisms.

## 9. Introduction of retardant (vaccine)

One admits that even the spatially independent smallpox model (3.1) is stultifying, and the space-time model (7.1) is worse. Yet, especially for the energetic computationalist/theorist, we need to address the issue of retardant (as in forest-fire models), or shall we say: vaccination.

For discrete models exemplified in Figures 3,5 vaccination is conceptually simple: One may simply deposit “colors” at vaccination positions, or somehow affect whole regions with vaccine. In the fire models, this procedure would be as computationally straightforward as it is

in fire-fighting practice; namely, one just drops retardant at various locations. We are not saying that retardant *strategy* is trivial; instead, we mean that the computational intricacies are easy. In fact, it is one of the present authors' research avenues to investigate the retardant/vaccine strategies as relate to the emergence of fractal infection boundaries (such as the variegated fire boundary of the upper-right of Figure 3).

[ADD: Simple combinatorics of discrete fire model with retardant.]

As for actual disease models, Figure 9 shows what the practicing epidemiologist confronts in continuum approaches to smallpox vaccination.

$S_i(t)$ = Susceptibles of immune status, $i \in 1, 2$ $V_i(t)$ = Vaccinated susceptibles of immune status, $i \in 1, 2$ $I_{ij}(t)$ = Infecteds of immune status, $i \in 1, 2$ , disease state, $j \in 1, 2, 3$ $X_i(t)$ = Vaccinated infecteds of immune status, $i \in 1, 2$ $R_i(t)$ = Recovered of immune status, $i \in 1, 2$ and $\mu_i$ = Rate of death by immune status, $i \in 1, 2$ $\Lambda_i$ = Rate of infection for given immune status, $i \in 1, 2$ $\nu_i$ = Rate of vaccination for given immune status, $i \in 1, 2$ $\theta$ = Vaccine efficacy factor $\bar{o}_i$ = Rate a vaccine - associated mortality, $i \in 1, 2$ $\gamma_{j,j}$ = Rate of disease progression for $i \in 1, 2$ and $j \in 1, 2, 3$ $\pi_i$ = Rate of disease progression among vaccinated infecteds, $i \in 1, 2$ $\rho_i$ = Rate of recovery among vaccinated infecteds, $i \in 1, 2$ $\delta_{i,j}$ = Rate of death due to disease for $i \in 1, 2$ and $j \in 1, 2, 3$
--

**Figure 10:** Typical parameter assignments for the inclusion of vaccination terms.

Then a typical smallpox system subject to the parameters of Figure 9 is shown in Figure 10.

$$\begin{aligned}
\frac{dS_i(t)}{dt} &= -\Lambda_i(t)S_i(t) - \mu_i S_i(t) - v_i S_i(t) \\
\frac{dV_i}{dt} &= \sum v_i S_i(t) - \Lambda_i \theta(t) V_i - (\phi_i + \mu_i) V_i \\
\frac{dI_{i,1}}{dt} &= (\sum \Lambda_i(t) S_i(t) + \sum \Lambda_i \theta(t) V_i) - v_i I_{i,1} - (\gamma_{i,1} + \mu_i) I_{i,1} \\
\frac{dX_i}{dt} &= \sum v_i I_{i,1} - \pi_i X_i - \rho_i X_i - (\phi_i + \mu_i) X_i \\
\frac{dI_{i,2}}{dt} &= \gamma_{i,1} I_{i,1} - (\gamma_{i,2} + \mu_i + \delta_{i,2}) I_{i,2} \\
\frac{dI_{i,3}}{dt} &= \gamma_{i,2} I_{i,1}(t) + \pi_i X_i - (\gamma_{i,3} + \mu_i + \delta_{i,3}) I_{i,3} \\
\frac{dI_{i,4}}{dt} &= \gamma_{i,3} I_{i,3}(t) - (\gamma_{i,4} + \mu_i + \delta_{i,4}) I_{i,4} \\
\frac{dR_i}{dt} &= (\gamma_{i,4} I_{i,4} + \rho_i X_i) - \mu_i R_i
\end{aligned}$$

**Figure 11:** A vaccination-relevant smallpox continuum system.

As if the system of Figure 11, with parameters of Figure 10, is not complex enough, a full space-time model should include the spatial-diffusion terms and contact-rate refinements as we have discussed, e.g. for system (7.1). Beyond these complications, we have the issues of commuter algebra, neighborhood- and behavioral issues.

## 10. Medical and public-health issues

[ADD: Discussion of how the mortality and other parameters in the smallpox model (3.1) become more important for long-duration epidemics, or when latency is enormous (HIV), and so on, admitting that in our microscopic presentation for Figure 5 and subsequent text, we ignored such important parameters.]

[ADD: describe here how various diseases differ greatly in their specific parameters  $\beta, \gamma$  and

mobility/contact probability issues.]

[ADD: Perhaps more details on smallpox parameters...maybe a table?]

[ADD: Address the fact that for some such as AIDS models, infection rate is not  $\beta SI$  but  $\beta S(I/(S + I))$ , on the idea that what matters is the fraction of the population is infected...related to the notion that symptomatic individuals will not generally infect...]

[ADD: Some scholarship on logistic-epidemic models, whereby long-term epidemics involve also the carrying capacity of the population, and other demographics.]

[ADD: Remarks on SIS models, whereby recovered can again become infected, and so on.]

## 11. Future directions

We have endeavored to provide pedagogy to convey how the theoretician—or the computationalist—may develop models, including full space-time models and even vaccination scenarios, whether in discrete or continuum modes. Needless to say, such pedagogy leaves many stones unturned. We end by summarizing some research directions:

- We have intimated that even simple discrete epidemic models can give rise to (experimentally) fractal survivor sets. Can the fractal dimension be a diagnostic quantity? E.g., can one determine the character of a (spent) forest fire by analyzing the topology of the (green) survivors? Certainly such mathematical expedients are in practice far safer (after a conflagration) than analyzing *during* the epidemic. The important principle here can be stated: Discrete models may be capable of providing not only prevention, but *diagnostic* tools with which to assess disease properties *a posteriori*, that is, after the conflagration/epidemic has passed.
- Do we not expect epizootic waves as formal solutions to smallpox-like systems such as (7.1)? If so, there are implications for bioterror: Meaning, situations with a spatially-sharp attack and, depending on the disease, rapid epidemic.
- What about the fractal dimension of the infection “boundary” in such as Figures 3,5? It is one of the research avenues of the present authors (separate treatment) to connect fractal-boundary effects with vaccination strategies. To foreshadow such research: It appears optimal, with limited vaccine, to *vaccinate preferentially near boundaries of high fractal dimension*.
- How do we analyze *scale-free* networks with respect to the pedagogical ideas herein? We note that scale-free networks have achieved an intense, modern vogue [ ] [ ], even in regard to computer-virus epidemics. In particular, the collision model of Figure 7 must accordingly be modified if collisions are expected in a scale-free fashion. For example, if the threatening infected (red) disks are preferentially connected somehow to susceptible (green) disks with *a priori* density  $k^{-\mu}$  from  $k$  connections, then all of the

contact algebra needs be modified. This dilemma is, of course, related to the problem of behavioral contact and geometrical-neighborhood effects.

## **Acknowledgments**

We are indebted to...

## **References**

[ADD: A great deal of references we already have, but need to sort out and prioritize.]